Tracking atrazine degradation in soil combining 14C-mineralisation assays and compound-specific isotope analysis

Sara Gallego, Rungroch Sungthong, Benoît Guyot, Adrien Saphy, Marion Devers-Lamrani, Fabrice Martin-Laurent, Gwenaël Imfeld

Chemosphere 363 (2024) 142981

Contents lists available at ScienceDirect

Chemosphere

journal homepage: www.elsevier.com/locate/chemosphere

Tracking atrazine degradation in soil combining ^{14}C-mineralisation assays and compound-specific isotope analysis

Sara Gallego [a], Rungroch Sungthong [b], Benoît Guyot [b], Adrien Saphy [b], Marion Devers-Lamrani [a], Fabrice Martin-Laurent [a], Gwenaël Imfeld [b,*]

[a] INRAE, Institut Agro Dijon, Université de Bourgogne Franche-Comté, Agroécologie Dijon, France
[b] Institut Terre et Environnement de Strasbourg, Université de Strasbourg/EOST/ENGEES, CNRS UMR 7063, Strasbourg, F-67084, France

HIGHLIGHTS

- Atrazine mineralisation and degradation in soil bioaugmented with bacterial isolates.
- ^{14}C-atrazine residues mass balance were combined with compound-specific isotope analysis.
- Atrazine mineralisation in soil experiments ranged from 10% to 40%.
- Atrazine degradation was determined using CSIA in water and solvent-extractable fractions.
- Monitoring atrazine transformation in soil and optimizing bioaugmentation for remediation.

GRAPHICAL ABSTRACT

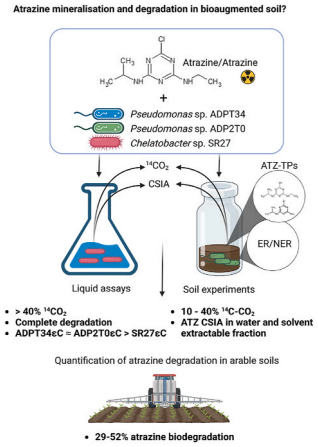

ARTICLE INFO

Handling editor: Keith Maruya

Keywords:
Herbicide
Atrazine
Soil
Bioaugmentation
Degradation
Mineralisation
CSIA

ABSTRACT

The quantification of pesticide dissipation in agricultural soil is challenging. In this study, we investigated atrazine biodegradation in both liquid and soil experiments bioaugmented with distinct atrazine-degrading bacterial isolates. This was achieved by combining ^{14}C-mineralisation assays and compound-specific isotope analysis of atrazine. In liquid experiments, the three bacterial isolates mineralised over 40% of atrazine, demonstrating their potential for extensive degradation. However, the kinetics of mineralisation and degradation varied among the isolates. Carbon stable isotope fractionation was similar for *Pseudomonas* isolates ADPT34 and ADP2T0, but slightly higher for *Chelatobacter* SR27. In soil experiments, atrazine primarily degraded into atrazine-desethyl, while atrazine-hydroxy was mainly observed in experiments with SR27. Atrazine mineralisation in soil by ADPT34 and SR27 exceeded 40%, whereas ADP2T0 exhibited a mineralisation rate of 10%. In experiments with ADPT34 and SR27, atrazine ^{14}C-residues were predominantly found in the non-extractable fraction, whereas they accumulated in the extractable fraction in the experiment with ADP2T0. Compound-

* Corresponding author. Institut Terre et Environnement de Strasbourg (ITES), Université de Strasbourg/EOST/ENGEES, CNRS UMR 7063, F-67084, Strasbourg, France.
E-mail address: imfeld@unistra.fr (G. Imfeld).

https://doi.org/10.1016/j.chemosphere.2024.142981
Received 3 June 2024; Received in revised form 24 July 2024; Accepted 29 July 2024
Available online 30 July 2024

specific isotope analysis (CSIA) relies on changes of stable isotope ratios and holds potential to evaluate herbicide transformation in soil. CSIA of atrazine indicated atrazine biodegradation in water and solvent extractable soil fractions and varied between 29% and 52%, depending on the bacterial isolate. Despite atrazine degradation in both soil fractions, a significant portion of atrazine residues persisted, depending on the bacterial degrader, initial cell concentration, and mineralisation and degradation rates. Overall, our approach can aid in quantifying atrazine persistence and degradation in soil, and in optimizing bioaugmentation strategies for remediating soils contaminated with persistent herbicides.

1. Introduction

Soil contamination by pesticide residues is a widespread issue that jeopardises the ecological and chemical status of soil and aquatic ecosystems, thereby threatening human health (Mateo-Sagasta et al., 2017). While pesticides and their transformation products (TPs) can leach from the soil into surface and groundwater, several pesticides and their TPs can persist for several decades in soil (Anagnostopoulou et al., 2022). However, evaluating the extent and pathways of pesticide degradation in soil is often out of reach (Fenner et al., 2013). Conventional monitoring approaches often cannot distinguish between truly recalcitrant pollutants and cases where degradation is too slow to be effectively monitored over time (Höhener et al., 2022), especially when information about transformation pathways is limited (Singh et al., 2018). To address this challenge, traditional radiorespirometry using radiotracer techniques under controlled conditions can be combined with compound-specific isotope analysis (CSIA) to monitor the degradation of persistent pesticides, such as atrazine, in soil.

Atrazine (ATZ) is a widely used chlorine s-triazine herbicide that can accumulate in soil. Despite being banned in all European countries decades ago, ATZ and its main TPs are still frequently detected in agricultural soils and groundwater. The persistent presence of ATZ is due to its extensive use for eradicating broadleaf weeds from corn crops and its chemical stability (Jablonowski et al., 2009; Riedo et al., 2021). The dissipation of ATZ in soil, marked by the reduction in ATZ concentrations, is driven by concurrent degradative processes, including both abiotic and biotic transformation of the ATZ molecule, and non-degradative processes, such as leaching, runoff, sorption and aging. Aging represents the gradual physical entrapment of ATZ within soil microsites over time.

In most soils, only biodegradation can achieve the complete mineralisation of ATZ to inorganic derivatives such as CO_2. However, biodegradation may generate toxic TPs that can persist as residues for decades. ATZ biodegradation in soil often follows the *N*-dealkylation pathway, leading to ATZ-deisopropyl and ATZ-desethyl (Shapir et al., 2007). ATZ-desethyl is more mobile than ATZ and remains herbicidal (LeBaron et al., 2008). Alternatively, ATZ is degraded through the hydroxylation pathway, leading to ATZ dehalogenation and the formation of less harmful hydroxy-ATZ (Mandelbaum et al., 1993). Monitoring both ATZ mineralisation, which directly evidences the elimination of ATZ residues, and ATZ biodegradation, the primary degradative route, is crucial for evaluating the risks associated with ATZ residues in soil.

Radiorespirometric analysis using ^{14}C-ATZ has been used for the sensitive quantification of ATZ distribution and mineralisation in soil microcosms (Kruger et al., 1993). ATZ mineralisation is typically traced through measuring $^{14}C–CO_2$ emissions from ^{14}C-ATZ while extractable and non-extractable residues can be quantified from the radioactivity remaining in soil (Jablonowski et al., 2013). The use of ^{14}C-ATZ allows the sensitive follow-up of ATZ distribution and transformation in soil fractions at environmentally-relevant concentrations (De Souza et al., 2022). However, due to the inherent risks associated with radioisotopes, radiorespirometric measurements to assess ATZ mineralisation are confined to small-scale laboratory experiments under controlled conditions, which may not accurately reflect field conditions.

Complementarily, compound-specific isotope analysis (CSIA) relies on changes in natural abundance of stable isotopes of elements (e.g., $\delta^{13}C$, $\delta^{15}N$) in pollutant molecules (Hofstetter et al., 2024). CSIA holds potential to evaluate the occurrence, pathway and extent of ATZ degradation in agricultural soil (Arar et al., 2023; Drouin et al., 2021; Torrentó et al., 2021). Pesticide CSIA can help differentiate degradative processes, involving molecular bond cleavage, from nondegradative processes leading to a decrease in ATZ concentration in soil (Elsner and Imfeld, 2016). In the course of degradation reactions that result in the cleavage of molecular bonds, bonds involving lighter isotopes (e.g., ^{12}C) tend to break at slightly faster rates compared to those involving heavier isotopes (e.g., ^{13}C). This can result in changes in the isotope ratios within the remaining, nondegraded fraction of pesticides in soil. Consequently, the use of ATZ CSIA can help to evidence ATZ transformation in soil and to quantify ATZ degradation when the corresponding reference isotope fractionation values (ε) are available.

Previous reference CSIA studies in laboratory experiments examined isotopic fractionation associated with bacteria harbouring the *atzA* and *trzN* genes (Meyer et al., 2009) and with bacterial cell-free extracts (Chen et al., 2022; Ehrl et al., 2018). These studies, conducted with pure strains and in liquid media, indicated that isotope fractionation of ATZ is sensitive to rate-limiting transport through the cell membrane and to bioavailability restriction at low ATZ concentration. Recently, the isotope effects for ATZ degradation by groundwater-derived cultures was examined with CSIA (Arar et al., 2023). However, reference experiments to evaluate the potential of CSIA for monitoring ATZ transformation in ATZ-contaminated soils over time are currently missing. This is mainly due to low concentrations and analytical difficulties associated with pesticide CSIA from soil samples, including low extraction recoveries and high matrix effects (Elsner and Imfeld, 2016; Höhener et al., 2022).

The aim of this study was to examine and compare the mineralisation and degradation of atrazine (ATZ) in arable soil bioaugmented with different ATZ-degrading bacterial isolates. Reference liquid assays and soil experiments were conducted with and without bioaugmentation using well-characterized ATZ-degrading bacterial isolates. Mineralisation assays with ^{14}C-labelled ATZ were combined with CSIA of ATZ to evaluate ATZ degradation in both extractable and non-extractable soil fractions. We hypothesized that (i) ATZ mineralisation and degradation in soil primarily depend on the bacterial isolate used for bioaugmentation, and (ii) evaluating ATZ mineralisation and degradation in both extractable and non-extractable fractions provides additional insights into the persistence of ATZ residues in bioaugmented soil.

2. Materials and methods

2.1. Chemicals

ATZ (2-chloro-4-ethylamino-6-isopropylamino-1,3,5-triazine; purity >99%) was provided by Syngenta, Switzerland. ATZ labelled with ^{14}C on the *s*-triazine cycle (radiochemical purity >99%; specific activity 246 mCi mmol^{-1}), deuterated labelled isotope of atrazine used as standard (ATZ-d5, purity >99%), and HPLC-grade solvents with a purity >99.9%, including methanol, dichloromethane, acetonitrile, ethyl acetate, and pentane, were procured from Sigma-Aldrich, St. Louis, USA.

2.2. Selection and cultivation of bacterial ATZ degraders

Two *Pseudomonas* isolates [ADPT34 (Devers et al., 2008) and ADP2T0 (unpublished)] isolated from a herbicide spill site (Mandelbaum et al., 1995), and *Chelatobacter* isolate SR27, isolated from a maize crop rotation treated with herbicide in Citeaux (France) (Rousseaux et al., 2003), were selected based on their distinct ATZ degrading genetic repertoires. The genes *atzABCDEF* are located on the plasmid pADP of ADPT34 and on the bacterial chromosom of ADP2T0. Isolate SR27 possesses genes *atzABC* and *trzD*. All three isolates possess AtzA as the primary degrading enzyme responsible for initiating the transformation of ATZ through dechlorination, ultimately leading to the formation of ATZ-hydroxy.

The bacterial isolates were grown separately in a mineral salt medium (Billet et al., 2019), containing 1 g L^{-1} citrate and 100 mg L^{-1} ATZ as a sole source of carbon, nitrogen, and energy (Devers et al., 2005). The liquid cultures were incubated in the dark at 28 °C on an orbital shaker at 120 rpm. Bacterial cells collected at the exponential phase were washed thrice using KNAPP buffer (Devers et al., 2004), collected by centrifugation at 5000 *g* for 10 min and resuspended for ATZ mineralisation and degradation assays.

2.3. ATZ mineralisation and degradation in liquid medium

2.3.1. ATZ mineralisation assays

A radiorespirometry assay was conducted to assess the ATZ mineralisation of the isolates. The ^{14}C-labelled and non-radioactive ATZ were dissolved in methanol and added (0.1% methanol; v/v) to triplicate 25 mL tubes with 10 mL of KNAPP buffer (1 g L^{-1} KH_2PO_4, 1 g L^{-1} K_2HPO_4, 4 mg L^{-1} $FeCl_3$, and 40 mg L^{-1} $MgSO_4$) to reach a final ATZ concentration of 5 mg L^{-1}, equivalent to 60.4 bq mL^{-1}. The tubes were agitated to facilitate the volatilization of methanol. The OD_{600nm} from ADPT34, ADP2T0 and SR27 isolates collected in KNAPP buffer was measured, and the concentrations were adjusted for incubation across a range of final cell densities: 0.001, 0.005, 0.01 or 0.05 OD_{600nm} mL^{-1}. Each tube was placed in an airtight flask, with an alkali trap (5 mL of 0.2 M NaOH) capturing the $^{14}CO_2$. The alkali trap was replaced regularly (Fig S1). Flasks were incubated at 28 °C on a rotary shaker at 120 rpm.

2.3.2. ATZ degradation assays

Bacterial isolates ADPT34, ADP2T0 and SR27 were inoculated, respectively, with final $OD_{600\ nm}$ of 0.01 ($1.71{\cdot}10^8 \pm 3.31{\cdot}10^7$ cells mL^{-1}), 0.05 ($3.40{\cdot}10^7 \pm 2.28{\cdot}10^7$ cells mL^{-1}) and 0.05 mL^{-1} ($8.42{\cdot}10^7 \pm 1.17{\cdot}10^7$ cells mL^{-1}) in 250 mL flasks containing 50 mL of KNAPP buffer and 5 mg L^{-1} ATZ. The cultures were incubated at 28 °C at 120 rpm. ATZ degradation experiments were conducted in five replicates, with a parallel series of noninoculated liquid controls. The culture broth was collected at ≥ 8 time points during ATZ degradation, from the lag phase up to early stationary phase, before centrifugation at 8000 *g* for 10 min. The supernatant was filtered through a 0.2 μm membrane filter. The filtrate was stored at −20 °C before ATZ quantification and CSIA to retrieve the carbon stable isotope fractionation value (ε_C) associated with ATZ degradation by ADPT34, ADP2T0 and SR27.

2.4. ATZ mineralisation and degradation in soil microcosm experiments

Clay-loam topsoil subsamples, each consisting of 3–5 subsamples from the first 15 cm of topsoil, were collected from various locations within the park of the INRAE experimental station in Bretenières, Côte d'Or, France (47°14′16.4"N - 5°05′54.9"E) and combined in a single representative soil sample (Hussain et al., 2013). The nonsterile soil was sieved through 4 mm mesh, thoroughly homogenized and stored at 4 °C. Soil characteristics are provided in Table 1.

Triplicate soil microcosm bioaugmentation experiments were conducted to monitor the mineralisation of ^{14}C-ATZ (Fig. 1). The isolates ADPT34, ADP2T0, and SR27 were individually introduced into the microcosms, while the control experiments were not bioaugmented. The soil microcosms consisted of 50 g of dry soil in 125 mL vials placed in airtight jars containing a vial filled with water to maintain the water content (Soulas, 1993). Each experiment was spiked with ATZ at a concentration of 5 mg kg^{-1}, reflecting typical environmental concentrations in soil following field application, which usually range from 1 to 9 kg ATZ ha^{-1} (Tappe et al., 2002). The ATZ stock solution (0.25 mg of ^{14}C-labelled and non-radioactive ATZ) was mixed in 100 μL of methanol and added into 5 g of soil (dry weight) to reach a final concentration of 36.4 bq g^{-1}. The soil was left overnight until complete methanol evaporation (Fig. 1). The remaining soil (45 g) was added and thoroughly homogenized with the spiked soil. The soil water content was adjusted to 50% of its water holding capacity (WHC). The soil microcosms were preincubated for seven days to account for ATZ sorption.

Table 1
Characteristics of the soil (Bretenière, France) used in soil microcosm experiments.

Parameter	Measured value
pH	7.6 ± 0.2
Proportion of sand/silt/clay (%)	24 ± 2.4/41 ± 3.7/35 ± 2.4 (clay loam)
Soil organic matter (g kg^{-1})	65.2 ± 5
Total organic carbon (g kg^{-1})	37.7 ± 3
N–NH_4^+ (mg kg^{-1})	6.1 ± 0.6
N–NO_3^- (mg kg^{-1})	12 ± 1.2
Cationic exchange capacity (meq kg^{-1})	261 ± 18.3

Based on the initial performance assessment with various cell concentrations, the soils were inoculated with cell suspension of 10^9 cells g^{-1} of soil for ADPT34, and 10^6 cells g^{-1} for ADP2T0 and SR27 in KNAPP buffer to achieve 70% of the soil WHC. The time of bacterial inoculation is referred to below as Day 0. KNAPP buffer was added into the control experiment to reach 70% of the WHC. The alkali trap was replaced at each sampling day (Fig. 1).

At the end of the incubation period, a^{14}C mass balance of radioactivity in soil was established to quantify extractable residues (ER), non-extractable residues (NER) and the extent of mineralisation from trapped $^{14}CO_2$ residues.

To evaluate ATZ biodegradation in soil, an additional set of five replicate soil microcosms was established. Each microcosm contained 5 mg kg^{-1} of non-radioactive ATZ, following the same procedure used for the ^{14}C-labelled ATZ microcosms (Fig. 1). Sampling was conducted based on degradation kinetics, using a sacrificial approach with 6, 8, and 9 time points for ADPT34, ADP2T0, and SR27, respectively (Fig. 1). All soil microcosms were incubated at 25 °C, maintained in darkness, within airtight respirometer jars containing a water-filled plastic vial to maintain humidity level (Soulas, 1993). The incubation period lasted for 35 days (ADPT34), 50 days (ADP2T0), and 29 days (SR27).

2.5. ATZ analysis

2.5.1. ATZ extraction

For experiment conducted with liquid medium, ATZ was extracted using a liquid-liquid extraction procedure (Gilevska et al., 2022). Briefly, 10% (v/v) dichloromethane was added to each liquid sample, followed by vortexing for 20 s, shaking for 5 min, and sonicating for 5 min. The resulting extract was transferred to a new amber glass tube. This extraction procedure was repeated three times. ATZ was then concentrated by solvent evaporation under a gentle, slow stream of N_2 and resuspended.

For soil microcosms experiments, ATZ was extracted from soil using a two-step solid-liquid modified ultrasonic-assisted extraction and purification previously described (Barriuso et al., 2004; Gilevska et al., 2022). This method allows for the separate collection of ATZ in the fractions extractable with water and organic solvent. The water content was adjusted to 100% prior to extraction. In the first extraction step to collect the water extractable fraction, 10 mL g^{-1} of 0.01 M $CaCl_2$ was

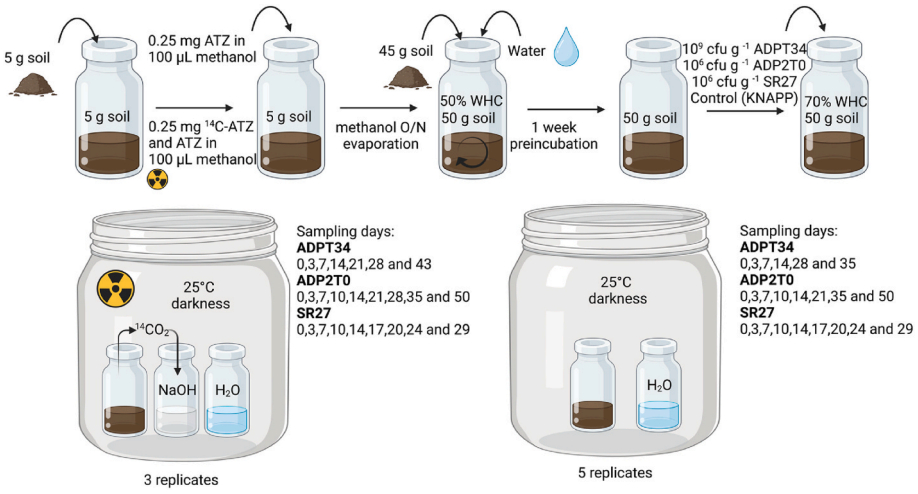

Fig. 1. Schematic diagram of soil microcosm experiments with ^{14}C-ring-labelled and non-radioactive ATZ. Soil bioaugmentation experiments were carried out with ATZ-degrading bacterial isolates ADPT34, ADP2T0 and SR27. The sampling times differed among the three isolate due to intrinsic variations in their mineralisation and degradation kinetics.

added to 5 g of soil dry weight. Samples were vortexed for 15 s and shaked at 600 rpm, then ultrasonicated for 5 min, vortexed for 1 min, and centrifuged for 10 min at 2000 rpm. The derived aqueous phase was collected. This procedure was repeated twice before ATZ extraction from the aqueous phase as described above. The remaining soil was extracted thrice with 3:1 pentane:dichloromethane (v/v, 1 mL g^{-1}) to collect the solvent extractable fraction, following the same procedure. The supernatants were combined and concentrated under a slow stream of N_2 until the last drop. ATZ was then resuspended in acetonitrile to achieve a final volume of 1 mL. Then 75 mg of anhydrous $MgSO_4$, to remove residual water, and 13 mg of primary-secondary amine (PSA bonded silica, Supelco P/N 52738) as a clean-up agent were added. The extracted samples were vortexed for 30 s before centrifugation for 5 min at 5000 *g*. The extracts were stored at −20 °C prior to ATZ analysis.

2.5.2. Quantification of ATZ and its transformation products

ATZ and its two main TPs in soil (Mudhoo and Garg, 2011), ATZ-hydroxy and ATZ -desethyl, were quantified in liquid and soil samples at all sampling times. Quantification was performed using ultra high-pressure liquid chromatography (UHPLC) (Dionex/Thermo Scientific UltiMate Dionex 3000) coupled with a triple quadrupole mass spectrometer (Thermo Scientific TSQ Quantiva), using an Accucore aQ column (100 × 2.1, particle size 2.6 µm). Water with 0.05% formic acid and acetonitrile with 0.1% formic acid were used as mobile phase. ATZ-d_5 was used as internal standards with every injection. Limit of quantification (LOQ) was 7 ng L^{-1} for all compounds (Supporting information (SI) for the detailed methods).

2.5.3. Mineralisation of ^{14}C-ATZ

For ATZ mineralisation assays, the collected alkali trap (5 mL) was mixed with 10 mL of Ultima Gold XR scintillation liquid (PerkinElmer, City, Country), and the radioactivity was determined in a Tri-CARB 2100 TR liquid scintillation counter (Beckman Coulter LS6500 Multi-Purpose Scintillation Counter, Beckman Coulter Inc., Ramsey, USA). The remaining ^{14}C- ATZ residues in each liquid medium was determined by mixing 1 mL of such medium with scintillation liquid for the radioactivity measurement.

To quantify the extractable residues (ER) of ATZ from soil samples, 65 mL of methanol was added to each 50 g dry soil sample. The mixture was thoroughly mixed and placed on a rotary shaker at 150 rpm for 24 h. After centrifugation for 10 min at 6000 *g*, the supernatant was collected, and 5 mL aliquots were mixed with scintillation liquid for radioactivity measurement. The remaining soil sample was then completely dried at ambient temperature. The ^{14}C non-extractable residues (NER) were quantified after combustion of 0.5 g of dried soil under O_2 flow at 900 °C for 4 min, with a biological oxidiser OX-500 (EG&G Instruments, France) (El-Sebai et al., 2005).

2.5.4. Compound-specific isotope analysis of ATZ

Carbon stable isotope composition ($\delta^{13}C$) of ATZ was measured using a Gas Chromatography Isotope Ratio Mass Spectrometry (GC-IRMS) system consisting of a TRACE™ Ultra Gas Chromatograph (Thermo-Fisher Scientific) coupled with a GC IsoLink/Conflow IV interface to an isotope ratio mass spectrometer (DeltaVplus, ThermoFisher Scientific) as described earlier (Gilevska et al., 2022). Briefly, ATZ standards with known and distinct isotopic compositions were injected every five samples to ensure measurement accuracy. The isotope compositions of the ATZ standards were calibrated relative to the Vienna Pee Dee Belemnite (VPDB) standard using Elemental Analyser Isotope Ratio Mass Spectrometry (EA–IRMS) (Flash EA IsoLink TM CN IRMS, Thermo Fisher Scientific). The calibration employed a two-point method with international reference materials AIEA600, USGS40, and USGS41. All isotopic measurements are reported in delta notation relative to VPDB (Coplen, 2011). The method detection limit, representing the lowest ATZ concentration within a linear interval of ±0.3‰ of the standard mean value with a reproducibility of $1\sigma < 0.3‰$, ($n \geq 3$), was determined as 6 ng of carbon on column, equivalent to 0.5 mg kg^{-1} of soil in this study. The liquid-liquid and liquid-solid procedures for ATZ extraction did not lead to significant isotope fractionation ($\Delta(^{13}C) \leq 0.5‰$) (Gilevska et al., 2022).

Given the sensitivity and accuracy of the method for carbon CSIA of ATZ from soil samples, this study focused on carbon CSIA to evaluate its applicability for soil samples with environmentally-relevant concentrations of ATZ. Considering the current extraction methodology, the available sample quantities from the microcosm experiments, and the analytical sensitivity, conducting nitrogen CSIA for ATZ in soil samples would necessitate an ATZ concentration in soil above 5 mg kg^{-1}, which is not environmentally relevant. Moreover, a precise and sensitive method for chlorine CSIA of ATZ from soil samples is currently unavailable, primarily due to the absence of certified standards and the lack of accuracy.

2.6. Data analysis

2.6.1. Mineralisation and degradation kinetics

The mineralisation of ^{14}C-ATZ over time was evaluated with the

sigmoidal Gompertz model using the SigmaPlot 13.0 software (SPSS):

$$y = A\ exp\left\{ - exp\left[\frac{\mu_m e}{A}(\lambda - t) + 1\right]\right\} \quad \text{Equation 1}$$

where λ is the lag phase, A is the maximum mineralisation extent (% of ^{14}C-ATZ initially added) and μ_m is the maximum mineralisation rate (% h^{-1} or d^{-1} of ^{14}C-ATZ initially added) (Hussain et al., 2013; Zwietering et al., 1990). ATZ degradation kinetics were calculated with Sigma Plot 15.0 using an exponential decay model ($C = C_i e^{-kt}$), where C is the concentration of ATZ (mg L^{-1}), t is the time (h or d), C_i is the concentration of ATZ at t_0 (mg L^{-1}), and k is the constant rate (h^{-1} or d^{-1}).

2.6.2. Mass balance of ^{14}C-ATZ residues

The mass balance of either ER and NER of ^{14}C-ATZ, was determined at the end of the mineralisation experiments by quantifying ^{14}C radioactivity recovered from liquid cultures and soil fractions, as described above.

2.6.3. Isotope fractionation and extent of biodegradation

The carbon isotope fractionation values (ε_C) relating a change in carbon stable isotope ratios (δ^{13}C) to the extent of ATZ degradation were derived from the Rayleigh equation, without forcing the regression through the origin (Scott et al., 2004):

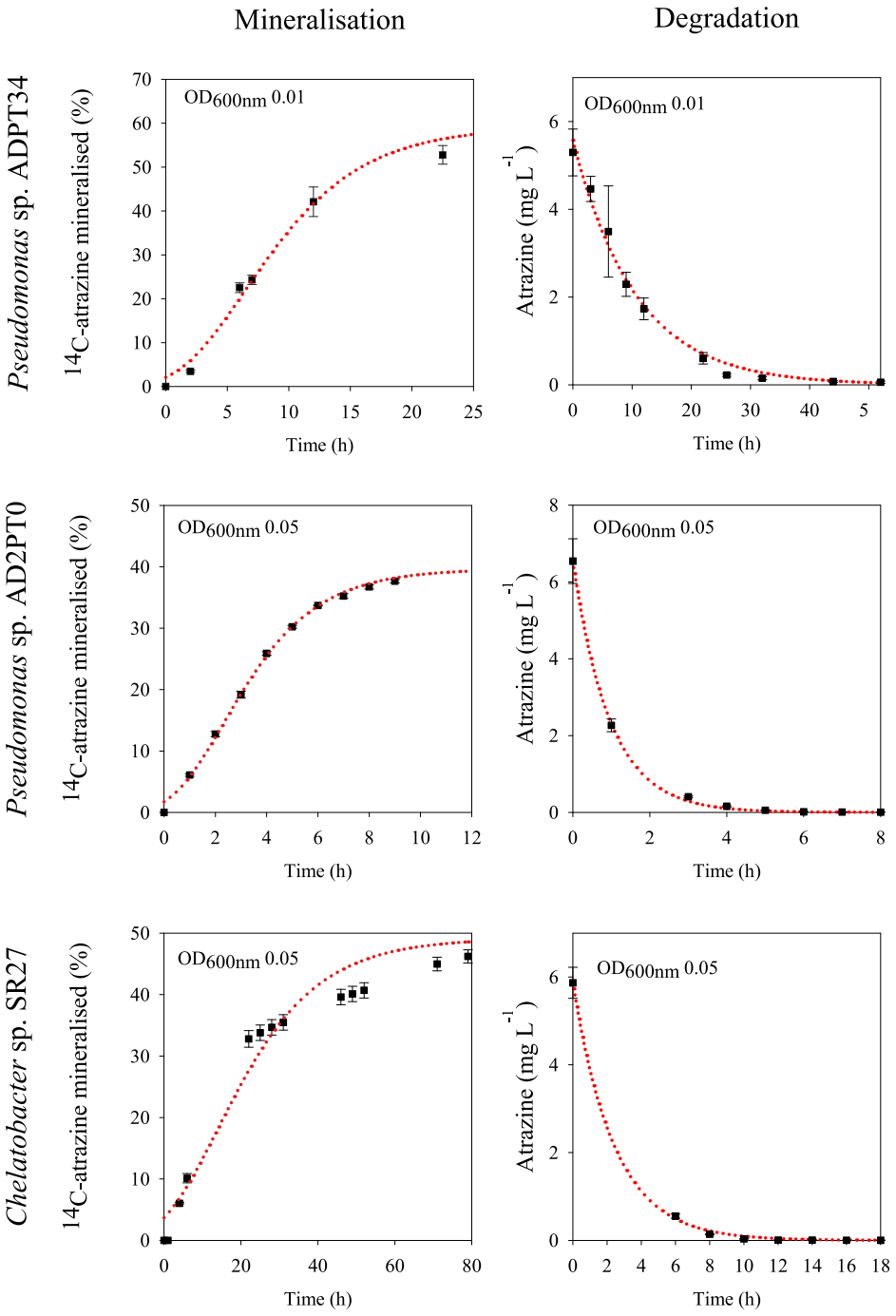

Fig. 2. Mineralisation and degradation of atrazine (ATZ) in liquid assays with ATZ-degrading bacterial isolates ADPT34, ADP2T0, and SR27. The curves represent sigmoidal Gompertz models for the mineralisation assays and exponential decay models for the degradation. Error bars indicate the standard deviation (±1σ) of the mean values, derived from replicate mineralisation (n = 3) and degradation (n = 5) experiments for each isolate.

$$ln\left(\frac{\delta^{13}C_t+1}{\delta^{13}C_0+1}\right)=\varepsilon_C\times ln\left(\frac{C_t}{C_0}\right) \quad \text{Equation 2}$$

where $\delta^{13}C_0$ and $\delta^{13}C_t$ represent the carbon stable isotope signature of ATZ at time 0 and t of the degradation, respectively, C_t is the fraction of remaining pesticides at time t, and C_0 is the initial ATZ concentration.

The extent of ATZ biodegradation (%) in soil microcosms was calculated using ε_C values determined in degradation assays in liquid media according to equation (3).

$$B=\left(1-\left(\frac{\delta^{13}C_t+1}{\delta^{13}C_0+1}\right)^{\frac{1}{\varepsilon_C}}\right)\times 100 \quad \text{Equation 3}$$

3. Results and discussion

3.1. ATZ mineralisation and degradation in liquid medium and isotope fractionation

Different cell concentrations in liquid media were first tested in mineralisation assays to examine the degradation kinetics (SI, Fig. S1) and optimize the initial cell concentration. About 40% of the ^{14}C-ATZ was mineralised by ADPT34 and ADP2T0 after 12 h–200 h, depending on the cell concentration (SI Fig. S1a and b). After 70 h of incubation, SR27 mineralised from 1% to 45% of the ^{14}C-ATZ, depending on the initial cell concentration (SI, Fig. S1c). No significant ATZ degradation was observed in the noninoculated control experiment (SI, Table S2). Based on these results, mineralisation and degradation assays were conducted with 0.01 OD_{600nm} mL^{-1} ($1.7{\cdot}10^8 \pm 3.3{\cdot}10^7$ cells mL^{-1}) for *Pseudomonas* sp. ADPT34, and 0.05 OD_{600nm} mL^{-1} ($3.4{\cdot}10^7 \pm 2.3{\cdot}10^7$ cells mL^{-1}) for *Pseudomonas* sp. ADP2T0 and *Chelatobacter* sp. SR27 ($8.4{\cdot}10^7 \pm 1.2{\cdot}10^7$ cells mL^{-1}).

The results of the mineralisation experiments in liquid media indicated a rapid but incomplete mineralisation of ATZ residues. The pattern of ^{14}C-ATZ mineralisation displayed a brief lag phase, followed by a peak of ATZ mineralisation exceeding 35% for all the isolates (Fig. 2). This corresponded to a mineralisation rates ranging from 1.2 ± 0.2 to 7.2 ± 0.1% h^{-1} for the three isolates. This range of mineralisation rates may reflect the distinct genetic repertoire of the ATZ-degrading isolates. *Chelatobacter* SR27, which possesses the *atzABC* and *trzD* genes, exhibited a slower mineralisation rate of ^{14}C-ATZ compared to the two *Pseudomonas* isolates, that have the complete *atzABCDEF* gene repertoire. The mass balance analysis conducted at the end of the incubation period revealed the recovery of $^{14}CO_2$ at 82 ± 5% for ADPT34, 52 ± 0.3% for ADP2T0, and 86 ± 4% for SR27, respectively (Table 2). Similar extents of mineralisation have been reported previously (Rousseaux et al., 2001; Satsuma, 2010).

Table 2
Kinetics of atrazine mineralisation (n = 3) and degradation (n = 5) in liquid assays by ATZ-degrading bacterial isolates ADPT34, ADP2T0, and SR27.

	ADPT34	ADP2T0	SR27
Mineralisation			
OD_{600nm} mL^{-1}	0.01	0.05	0.05
CFU mL^{-1}	$1.71{\cdot}10^8 \pm 3.31{\cdot}10^7$[a]	$3.40{\cdot}10^7 \pm 2.28{\cdot}10^7$	$8.42{\cdot}10^7 \pm 1.17{\cdot}10^7$
A [%]	59.9 ± 2.2	39.7 ± 0.1	49.4 ± 1.3
μ_m [% h^{-1}]	4.1 ± 1.0	7.2 ± 0.1	1.2 ± 0.2
λ [h]	0.9 ± 1.0	0.3 ± 0.1	0
Non-mineralised ATZ [%]	19.1 ± 1.2	11.30 ± 0.3	30.6 ± 6.1
A + non-mineralised ATZ	81.8 ± 5.0	51.67 ± 0.3	85.8 ± 3.5
Loss	18.2 ± 5.0	48.3 ± 0.3	14.2 ± 3.5
Degradation			
k [h^{-1}]	0.09 ± 0.01	1.04 ± 0.04	0.41 ± 0.02
Half-life [h]	8.5 ± 0.2	0.9 ± 0.02	2.1 ± 0.1
Initial degradation rate [mg L^{-1} h^{-1}]	0.5 ± 0.05	6.8 ± 0.35	2.4 ± 0.1
Isotope fractionation value (ε_C) [‰]	−1.82 ± 0.10[b]	−1.61 ± 0.10	−3.53 ± 0.31

[a] Uncertainties indicate standard deviations (±1σ) of the mean values.
[b] The uncertainties associated with ε_C values derived from the Rayleigh equation are expressed as 95% confidence intervals (±95% CI).

Although mineralisation of ^{14}C-ATZ residues was incomplete, ATZ was completely degraded by all isolates. ATZ degradation commenced immediately following its introduction in the culture medium and was completed within 52, 8, and 16 h for ADPT34, ADP2T0, and SR27, respectively (Fig. 2). The degradation rate constant (k) for ADP2T0 was up to ten times higher compared to SR27 and ADPT34 (Table 2). As as result, ATZ exhibited a shorter half-life with ADP2T0 compared to ADPT34. This difference aligns with the varying levels of adaptation of the two strains to ATZ mineralisation, with ADPT34 having undergone approximately 320 generations on ATZ medium (Devers et al., 2008) and ADP2T0 having undergone 120 generations (data not shown). Altogether, these results indicate that the taxonomy (Rousseaux et al., 2003), the ATZ-degrading genetic repertoire (Devers et al., 2007), and the level of adaptation to ATZ (Changey et al., 2011) are fundamental variables affecting both the extent and kinetics of ATZ mineralisation and degradation by ATZ degraders.

The carbon isotope fractionation values (ε_C) during ATZ degradation were similar for the two *Pseudomonas* isolates, ADPT34 and ADP2T0, but differed from those observed for *Chelatobacter* sp. SR27 (Table 2 and SI, Fig. S2). These ε_C values were consistent with those previously reported for biotic hydrolysis by the same strains (Meyer et al., 2009) and reflected a primary normal isotope effect. Both SR27 and ADP isolates possess the AtzA enzyme, which catalyzes the initial dichlorination step of ATZ to hydroxy-ATZ. However, the smaller carbon isotope fractionation for ADP2T0 and ADPT34 compared to SR27 suggests that isotope fractionation might be masked by slow steps that involve minimal or no isotope fractionation, such as mass transfer across the Gram-negative cell envelope (Chen et al., 2019; Ehrl et al., 2018), differing from the isotopically sensitive bond cleavage.

Small variations in isotope fractionation factors for the same enzymatic reaction can introduce minor uncertainty in quantifying ATZ biodegradation in soil using CSIA. However, in our soil bioaugmentation experiments, both the principal degradation pathway and the predominating degrading bacteria are well characterised. This allowed to estimate the extent of ATZ degradation in the soil bioaugmentation experiments using the ε_C values determined in degradation assays in liquid media (see equation (3) and section 3.4).

3.2. Mineralisation of ATZ in soil experiments

Over 40% of the ^{14}C-ATZ was mineralised in soil microcosms within 28 or 20 days after inoculation with 1×10^9 and 1×10^6 cells g^{-1} of ADPT34 and SR27, respectively (Fig. 3). Mineralisation experiments with lower cell concentrations showed significantly reduced mineralisation extents (<5.3%) (data not shown). This suggests that the initial bacterial inocula in soil should be above 1×10^9 cells g^{-1} for ADPT34 and 1×10^6 cells g^{-1} for SR27 to survive and overcome competition with indigenous microbiota. In contrast, ADP2T0 mineralised only 10.2 ± 3.6% of ^{14}C-ATZ 50 days after inoculation with 1×10^6, 1×10^7 or 1×10^8 cells g^{-1} of soil (SI, Fig. S3). Following a lag phase ranging from 0.1 ± 0.1 to 1.4 ± 0.5 days, mineralisation rates of 9.5 ± 1.3% d^{-1} (ADPT34), 4.1 ± 0.5% d^{-1} (SR27) and 0.30 ± 0.02% d^{-1} (ADP2T0) were observed (Table 3).

Overall, these results suggest that ADPT34 and SR27 may be more suitable for bioaugmentation in soil than ADP2T0. Although ADP2T0 demonstrated similar ATZ mineralisation capabilities in the liquid medium compared to the other bacterial isolates, it exhibited the lowest ATZ mineralisation in the soil bioaugmentation assay. This suggests that the extensive adaptation of ADP2T0 through reapeated exposure to ATZ had detrimental effects on its ability to acclimate to the soil environment. In soil, ADP2T0 likely faced less favorable selection pressure from ATZ and encountered competition with indigenous soil microbiota. This underscores the importance of selecting ATZ degraders with both

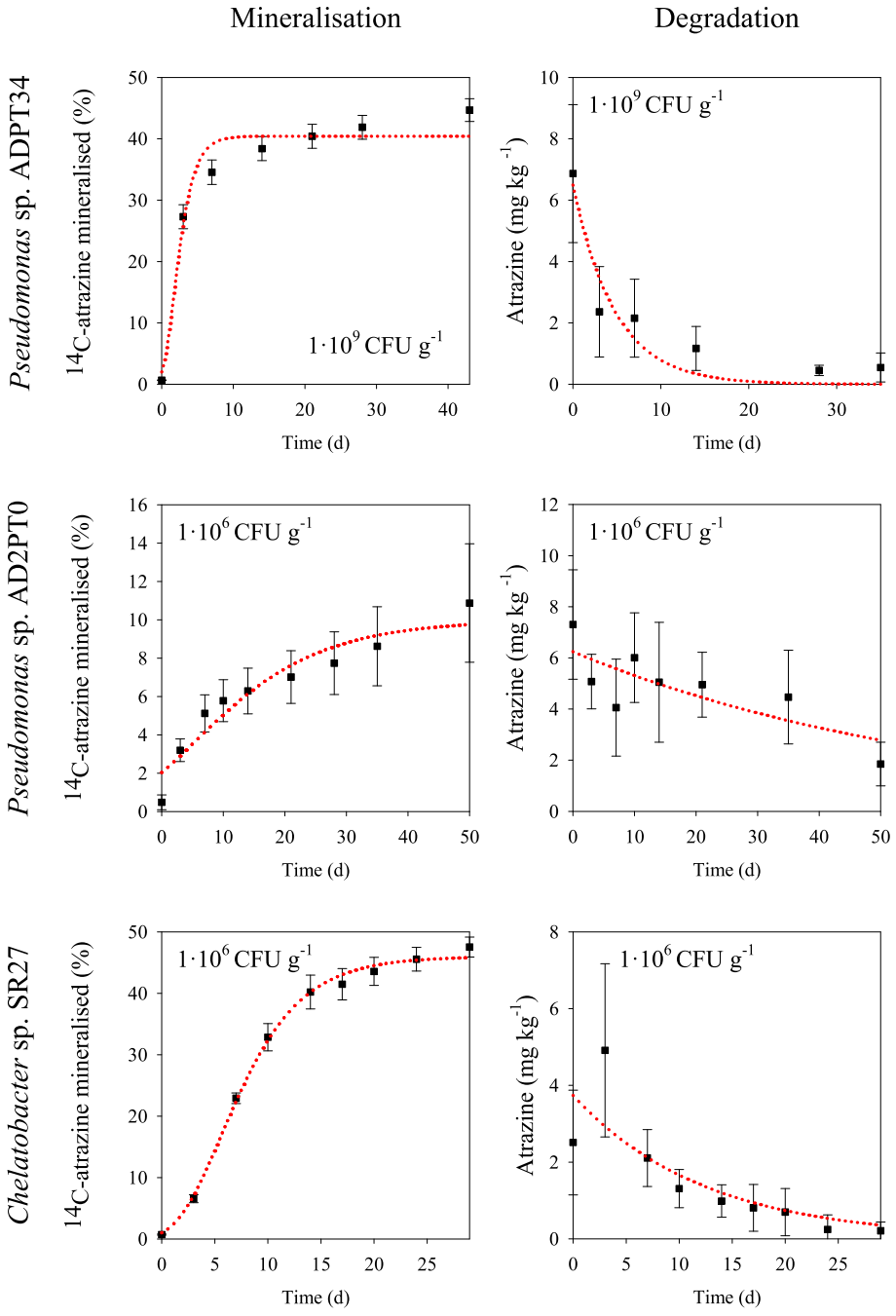

Fig. 3. Mineralisation and degradation of atrazine in soil experiments with atrazine-degrading bacterial isolates ADPT34, ADP2T0, and SR27. The curves depict the sigmoidal Gompertz models for mineralisation assays and exponential decay models for degradation. Error bars denote the standard deviation (±1σ) of the mean values derived from replicate mineralisation (n = 3) and degradation (n = 5) experiments for each bacterial isolate.

effective degrading abilities and the capability to compete with indigenous soil microbiota to maximise their bioremediation potential (Jia et al., 2021).

The mass balances revealed that over 64% of the ^{14}C-ATZ in experiments with ADPT34 and SR27 was recovered as $^{14}CO_2$ and $^{14}CO_2$ residues, encompassing ER, NER and ^{14}C-labelled biogenic residues. In contrast, only 35.4 ± 8.3% was recovered as $^{14}CO_2$ and $^{14}CO_2$ residues in experiments with ADP2T0. The contribution of ^{14}C biogenic residues may be significant, particularly when high cell densities are employed and substantial mineralisation rate is observed, as in the experiment with ADPT34. The discrepancy in ATZ mineralisation rates and formation of ^{14}C biogenic residues may also explain variations in ER and NER proportions among experiments.

In soil experiments with ADPT34 and SR27, extractable residues of ATZ accounted for approximately 10% of the total $^{14}CO_2$ recovered, whereas it was four to five times higher in the experiment with ADP2T0 (Table 3). This suggests that the degradation of ATZ residues in experiments with ADPT34 and SR27 primarily occurred within the extractable fraction, where ATZ likely exhibited higher bioavailability. In contrast, ATZ residues persisted in both ER and NER fractions in the experiment with ADP2T0, emphasising limited ATZ mineralisation.

Noteworthily, about one-third of ATZ residues were also recovered as NER in the experiment with SR27 (Table 3). This indicates that a significant fraction of ATZ residues may not be extractable from the soil, which is crucial to consider when evaluating ATZ dissipation based on concentration measurements. This NER fraction may vary depending on

Table 3
Kinetics of atrazine (ATZ) mineralisation in soil microcosm experiments with and without bioaugmentation with ATZ-degrading bacteria ADPT34, ADP2T0, and SR27, along with the control. ER: extractable residues, NER: non-extractable residues.

	Control	ADPT34	ADP2T0	SR27
CFU g^{-1}	–	10^9	10^6	10^6
A [%]	3.4 ± 2.5[a]	40.5 ± 1.9	10.2 ± 3.6	46.0 ± 1.8
μ_m [% d^{-1}]	-[b]	9.5 ± 1.3	0.3 ± 0.02	4.1 ± 0.5
λ [d]	–	0.14 ± 0.11	0	1.4 ± 0.5
A + ER + NER [%]	47.1 ± 14.7	64.3 ± 3.1	35.4 ± 8.3	77.9 ± 2.1
ER·(A + ER + NER)$^{-1}$ [%]	56.5 ± 10.5	10.0 ± 2.7	40.6 ± 3.4	8.1 ± 1.4
NER·(A + ER + NER)$^{-1}$ [%]	34.5 ± 11.4	20.5 ± 4.8	29.0 ± 2.0	30.8 ± 0.5
Loss	–	35.6 ± 3.1	64.6 ± 8.3	22.1 ± 2.1

[a] Uncertainties denote the standard deviation (±1σ) of the mean values derived from triplicate mineralisation experiments for each isolate and the control.
[b] As the data from the control experiment did not fit the Gompertz model, μ_m and λ parameters were not determined.

the extraction procedure and soil characteristics. Consequently, an apparent decrease of ATZ concentration in soil may not solely reflect its degradation but also its aging within soil components. Sorption and aging of ATZ and its TP in soil organic matter and minerals become substantial after a few weeks (Mudhoo and Garg, 2011; Park et al., 2004), and the significance of NER fraction may be contingent upon the activity of prevailing microbial degraders.

The loss in ^{14}C mass balance was higher than 20% for all experiment. This can be attributed to the volatilization of ^{14}C-ATZ, ^{14}C-TPs, and the loss of $^{14}CO_2$ upon opening the airtight respirometer jars to replace the alkali trap. This loss of ^{14}C-compounds became particularly significant when the mineralisation rates were high, as observed for ADP2T0 in the liquid medium, and increased with multiple sampling time points.

3.3. ATZ dissipation and transformation products in soil

In the experiments with ADPT34, ADP2T0, and SR27, ATZ dissipation in soil began immediately after its addition, showing a faster rate compared to the control experiment without bioaugmentation (Fig. 4). This indicates ATZ degradation in the bioaugmented soils. ATZ was predominantly present (>60%) in the water-extractable fraction in all experiments and throughout the investigation period (Fig. 4). This underscores the potential bioavailability and degradation of ATZ in the dissolved phase of the soil, although ATZ degradation is also possible in the solid, solvent extractable fraction of the soil (Barriuso et al., 2004). Interestingly, the proportion of ATZ in the water-extractable fraction was higher than that of ATZ residues extracted with methanol in the mineralisation assays. This may be attributed to the higher penetration of water with 0.01 M $CaCl_2$ into soil pores and its more effective disruption of hydrophobic interactions, leading to higher ATZ extraction efficiency with water despite its lower solubility in water (Barriuso et al., 2004).

The kinetics of ATZ dissipation were similar in experiments involving ADPT34 and SR27, which displayed dissipation rate constants (k) four to ten times higher than those in experiments with ADP2T0 (Table 4). As a result, the dissipation half-lives of ATZ in soil experiments with ADPT34 and SR27 were notably shorter than in the experiment with ADP2T0 (57 ± 9 days) (Table 4), with ATZ dissipation decreasing at an ATZ concentration of approximately 3 mg kg^{-1}. This indicates slower ATZ degradation in the experiment with ADP2T0, attributed to the lower initial cell concentration and declining ATZ bioavailability over time due to ATZ aging in the soil (De Jonge et al., 2004). This result is also consistent with the low ATZ mineralisation extents and rates in the experiment with ADP2T0 (Table 3).

ATZ degradation in soil may lead to the formation of more than 15 TPs (Singh et al., 2018). Among the most relevant ATZ TPs in soil are ATZ-desethyl and ATZ-hydroxy, which result from oxidative

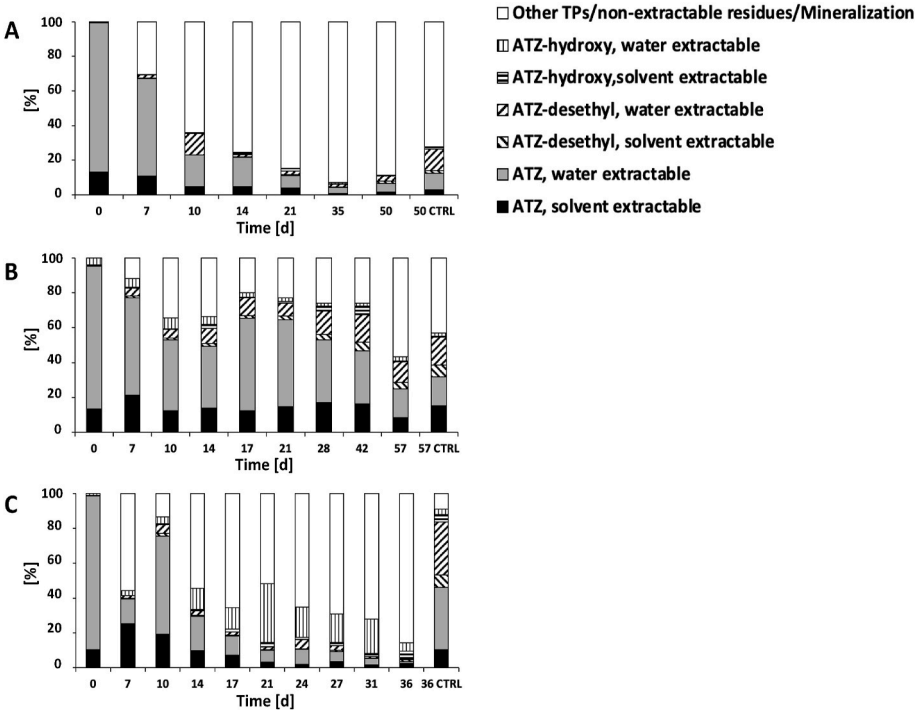

Fig. 4. ATZ, ATZ-hydroxy and ATZ-desethyl in both the water-extractable and the solvent-extractable fractions in bioaugmented soil experiments with ADPT34 (A), ADP2T0 (B), and SR27 (C). CTRL: Control experiment without inoculation.

Table 4
Kinetics of atrazine (ATZ) dissipation in soil microcosm experiments with and without bioaugmentation with ATZ-degrading bacteria ADPT34, ADP2T0, and SR27, along with the control.

	Control	ADPT34	ADP2T0	SR27
k [d^{-1}]	0.03 ± 0.007[a]	0.21 ± 0.05	0.02 ± 0.01	0.08 ± 0.02
Half-life [d]	36.7 ± 5.4	4.5 ± 0.5	57 ± 9	5 ± 0.3
Initial rate of degradation [mg kg^{-1} d^{-1}]	0.17 ± 0.07	1.4 ± 0.5	0.10 ± 0.04	0.30 ± 0.11

[a] Uncertainties denote the standard deviation (±1σ) of the mean values derived from replicate degradation experiments (n = 5) for each isolate and the control.

N-dealkylation and hydrolysis pathways, respectively (Mudhoo and Garg, 2011). In our soil experiments, ATZ biodegradation is expected to be the primary process, while abiotic hydrolysis of ATZ typically occurs due to its protonation in soils with a pH below 6.

The proportion of targeted ATZ TPs constituted more than 40% of the total mass of ATZ residues at the end of all experiments, with values reaching up to 76% for isolate SR27 (Fig. 4). This underscores significant ATZ degradation and the persistence of ATZ TPs in both bioaugmented and control experiments (Fig. 4), which is consistent with results of the mass balance of ^{14}C-residues (Table 3). ATZ-desethyl and ATZ-hydroxy were predominantly (>70%) found in the water extractable fraction, and their concentrations increased after 10 days. This can be attributed to their higher water solubility and weaker interactions of ATZ-hydroxy and ATZ-desethyl with soil constituents compared to ATZ. ATZ-hydroxy exhibits greater retention in soil compared to other TPs (Mudhoo and Garg, 2011). Given that chlorinated ATZ-desethyl remains herbicidal and is more mobile and toxic than ATZ-hydroxy (LeBaron et al., 2008; Shapir et al., 2007), it is imperative to consider the contribution of dealkylation versus hydrolysis pathways in soils.

ATZ-desethyl predominated in experiments with ADPT34 and ADP2T0, as well as in the control experiment without bioaugmentation, whereas ATZ-hydroxy was more prevalent in the experiment with SR27 (Fig. 4). This suggests that the formation of ATZ-desethyl primarily occurred due to the activity of indigenous soil bacteria, as observed in the control experiments. Specifically, both isolates of *Pseudomonas* and isolate SR27 of *Chelatobacter* can metabolize ATZ through a hydrolytic mechanism, involving the initial enzymatic step facilitated by AtzA enzyme leading to ATZ-hydroxy (De Souza et al., 1996; Shapir et al., 2007). The dominance and persistence of ATZ-hydroxy in the experiment with SR27 corresponded to the substantial amount (>30%) of ATZ residues recovered as extractable residues (ER) and non-extractable residues (NER) in the mineralisation experiments (Table 3), despite rapid ATZ degradation. This indicates that ATZ residues, including ATZ-hydroxy, degraded slowly in the SR27 experiment. ATZ-hydroxy may be excreted by the bacteria and temporarily stored in the soil as a coping mechanism to counteract its intracellular toxicity. In contrast, the degradation of ATZ-hydroxy was faster in experiments with ADPT34 and ADP2T0, although the overall mineralisation rate was slower in the ADP2T0 experiment.

Altogether, ATZ TPs transiently accumulated and degraded in both the bioaugmented and control experiments, with variations arising from the efficacy of ATZ-degrading isolates in soil. Nonetheless, degradation and aging of both ATZ and its TPs may largely vary over time, which complicates the accurate evaluation of ATZ degradation among other dissipation processes in agricultural soils. This underscores the challenges in predicting ATZ degradation pathways and extents solely based on ATZ concentration and TP profiles in both bioaugmented and natural soil. These challenges are expected to intensify during the evaluation of naturally occurring attenuation of ATZ under field conditions, as both non-degradative and degradative processes can concurrently affect concentrations of ATZ and its TPs in soil. Hence, additional approaches, such as compound-specific isotope analysis (CSIA) can provide direct means to evaluate ATZ degradation in soil without the need for TP quantification.

3.4. Quantification of ATZ degradation in soil using CSIA

Changes in the carbon stable isotope composition ($\Delta(^{13}C)$) of ATZ enabled the quantification of ATZ degradation using carbon isotope fractionation values (ε_C) obtained from ATZ biodegradation assays in liquid medium and applying Equation (3). Since the predominant isolate in soil bioaugmentation experiments was well-characterized, the corresponding ε_C values derived from each ATZ degradation assay with ADPT34, ADP2T0, and SR27 were employed. ATZ degradation in each soil experiments was estimated using the maximal $\Delta(^{13}C)$ observed in both the water and solvent-extractable fractions at sampling times that allowed the recovery of sufficient amounts of ATZ from both fractions for reliable CSIA (Table 5).

Significant changes in isotope ratios ($\Delta(^{13}C)$ >1‰) were observed in both the water and solvent-extractable soil fractions across all experiments at sampling times corresponding to 50%–90% of ATZ dissipation (Fig. 4 and Table 5). This confirmed ATZ degradation. Estimates of ATZ degradation extents, ranging from 29% to 52%, were consistent between the water and solvent-extractable fractions in all experiments (Table 5). Partial ATZ biodegradation in both fractions aligned with mineralisation assays (Table 3), indicating that ATZ residues persisted in both fractions across all experiments and over time. While these results indicate that ATZ degrade in both fractions, they also suggest that ATZ residues, including a significant proportion of ATZ, transiently accumulated in the extractable fraction of the soil.

Complementarily to mineralisation assays with radioisotopes under laboratory conditions, CSIA data underscored the potential for examining ATZ transformation under field conditions. The results showed that calculated ATZ degradation extents were generally lower than observed ATZ dissipation in soil (Fig. 4). This discrepancy can be attributed to ATZ aging in the soil, which may immobilize a fraction of ATZ that cannot be extracted with classical procedures and is less degradable due to its low bioavailability (Barriuso et al., 2004). Furthermore, the ε_C values used to estimate biodegradation were determined at high ATZ concentration and in liquid cultures, where mass transfer limitations are minimal (Ehrl et al., 2018). In our soil experiments, mass transfer limitations at low ATZ concentration may reduce isotope fractionation compared to liquid culture. As a result, the extent of biodegradation may be slightly underestimated, yielding

Table 5
Changes in carbon isotope composition ($\Delta(^{13}C)$) of atrazine (ATZ) and ATZ biodegradation extents in solvent and water extractable fractions in soil experiments with isolates ADPT34, ADP2T0 and SR27. Biodegradation extents [%] were calculated using equation (3) and the maximum $\Delta(^{13}C)$ at sampling times throughout the biodegradation experiments enabling reliable CSIA of ATZ in both soil fractions.

Isolate in soil experiment	Sampling time [d]	Max. $\Delta(^{13}C)$ [‰]		ATZ biodegradation [%]	
		Solvent	Water	Solvent	Water
Pseudomonas sp. ADPT34	10	1.1 ± 0.4[a]	1.2 ± 0.4	44–46[b]	44–46
Pseudomonas sp. ADP2T0	28	2.3 ± 0.4	1.6 ± 0.4	50–52	49–50
Chelatobacter sp. SR 27	17	2.9 ± 0.4	3.0 ± 0.4	29–36	31–36

[a] The error associated with the $\Delta(^{13}C)$ values was determined through error propagation using one standard deviation (±1σ) of the mean values obtained from five replicate experiments and from n ≥ 3 measurements for each sample at each sampling time.

[b] The ranges of biodegradation extents [%] were derived from the errors associated with the $\Delta(^{13}C)$ values and the isotope fractionation values (ε_C).

conservative estimates of ATZ degradation in soil.

CSIA data also revealed ATZ degradation in the solvent-extractable fraction, a phenomenon undetectable through mineralisation assays because ^{14}C-ATZ residues include both ATZ and its TPs. ATZ degradation in the solvent-extractable fraction can be attributed to the moderate sorption of ATZ to soil organic matter and weak interactions with soil minerals at a pH of 7.6 (Czaplicka et al., 2018). This may allow sufficient ATZ bioavailability within the solvent-extractable soil fraction for bacterial degradation of ATZ. However, this scenario may differ under field conditions. For legacy ATZ residues that have undergone decades of aging (Park et al., 2004), ATZ degradation in the solvent-extractable fraction is expected to be limited.

Given that the primary aim of this study was to evaluate the extent of degradation at environmentally relevant ATZ concentrations, focusing on the primary degradation pathway of biotic hydrolytic dechlorination, and considering that abiotic hydrolysis of ATZ is not expected under neutral conditions, estimates of biodegradation relied on carbon stable isotope data. However, multi-element CSIA, which includes elements such as Cl, C, and N, may provide a more comprehensive interpretation of ATZ transformation in soil (Torrentó et al., 2021). A combined approach using multi-element CSIA data may help differentiate between ATZ degradation pathways in soil, such as oxidative dealkylation, alkaline hydrolysis, acidic hydrolysis, and biotic hydrolysis.

Despite the analytical challenges associated with pesticide compound-specific isotope analysis (CSIA) due to their low concentrations in soil, this study demonstrates that ATZ transformation can be evaluated in soil experiments at environmentally relevant concentrations (0.5–5 mg kg^{-1}). This enhances predictive assessments of ATZ biodegradation in arable soil. ATZ transformation or persistence can be monitored over time in agricultural field soil using CSIA, provided a sufficient amount of ATZ (above 6 ng of carbon on column) can be extracted from soil samples, and reliable CSIA measurements can be made. However, further studies are required to assess ATZ concentrations at low levels and accounting for ATZ aging in soil.

4. Conclusion

Laboratory investigations into atrazine mineralisation and degradation in agricultural soil offer insights into transformation products and atrazine residue distribution in soil fractions, enhancing understanding of atrazine degradation and persistence. This study combined radiorespirometric analysis with ^{14}C-atrazine and degradation experiments using Compound-Specific Isotope Analysis (CSIA) in both liquid assays and soil, bioaugmented or not with distinct atrazine bacterial degraders. This approach enabled quantification of atrazine mineralisation, degradation, and transformation product formation over time in both extractable and non-extractable fractions of an agricultural soil. Our findings included reference mineralisation and carbon isotope fractionation experiments and values to evalute *in situ* degradation of persistent herbicides in soil, facilitating predictions of atrazine transformation under natural or bioaugmented conditions. Further investigations are needed to evaluate bioaugmentation feasibility and efficiency to eliminate persistent aged herbicides in arable soil and to estimate possible side-effects of bioaugmentation on the soil microbiome and on the soil heath.

CRediT authorship contribution statement

Sara Gallego: Writing – review & editing, Writing – original draft, Visualization, Validation, Methodology, Investigation, Formal analysis, Data curation, Conceptualization. **Rungroch Sungthong:** Writing – review & editing, Methodology, Investigation, Formal analysis, Conceptualization. **Benoît Guyot:** Writing – review & editing, Methodology, Formal analysis, Data curation. **Adrien Saphy:** Writing – review & editing, Validation, Methodology, Investigation, Formal analysis. **Marion Devers-Lamrani:** Writing – review & editing, Formal analysis, Data curation. **Fabrice Martin-Laurent:** Writing – review & editing, Validation, Supervision, Resources, Project administration, Investigation, Conceptualization. **Gwenaël Imfeld:** Writing – review & editing, Writing – original draft, Visualization, Validation, Supervision, Project administration, Methodology, Investigation, Funding acquisition, Formal analysis, Data curation, Conceptualization.

Declaration of competing interest

The authors declare no financial interests/personal relationships which may be considered as potential competing interests.

Data availability

Data will be made available on request.

Acknowledgements

This project was funded by the French National Research Agency (ANR) through grant number: ANR-18-CE04-0004-01, project DECISIVE. We would like to express our gratitude to Prof. Patrick Höhener (University of Aix-Marseille, France) for useful discussions and Nadine Rouard (INRAE Bourgogne Franche-Comté) for her technical support in radiorespirometric analyses.

Appendix A. Supplementary data

Supplementary data to this article can be found online at https://doi.org/10.1016/j.chemosphere.2024.142981.

References

Anagnostopoulou, K., Nannou, C., Evgenidou, E., Lambropoulou, D., 2022. Overarching issues on relevant pesticide transformation products in the aquatic environment: a review. Sci. Total Environ. 815, 152863 https://doi.org/10.1016/j.scitotenv.2021.152863.

Arar, M., Bakkour, R., Elsner, M., Bernstein, A., 2023. Microbial hydrolysis of atrazine in contaminated groundwater. Chemosphere 322, 138226. https://doi.org/10.1016/j.chemosphere.2023.138226.

Barriuso, E., Koskinen, W.C., Sadowsky, M.J., 2004. Solvent extraction characterization of bioavailability of atrazine residues in soils. J. Agric. Food Chem. 52, 6552–6556. https://doi.org/10.1021/jf040245l.

Billet, L., Devers, M., Rouard, N., Martin-Laurent, F., Spor, A., 2019. Labour sharing promotes coexistence in atrazine degrading bacterial communities. Sci. Rep. 9, 18363 https://doi.org/10.1038/s41598-019-54978-2.

Changey, F., Devers-Lamrani, M., Rouard, N., Martin-Laurent, F., 2011. In vitro evolution of an atrazine-degrading population under cyanuric acid selection pressure: evidence for the selective loss of a 47kb region on the plasmid ADP1 containing the atzA, B and C genes. Gene 490, 18–25. https://doi.org/10.1016/j.gene.2011.09.005.

Chen, S., Ma, L., Wang, Y., 2022. Kinetic isotope effects of C and N indicate different transformation mechanisms between atzA- and trzN-harboring strains in dechlorination of atrazine. Biodegradation 33, 207–221. https://doi.org/10.1007/s10532-022-09977-y.

Chen, S., Zhang, K., Jha, R.K., Chen, C., Yu, H., Liu, Y., Ma, L., 2019. Isotope fractionation in atrazine degradation reveals rate-limiting, energy-dependent transport across the cell membrane of gram-negative rhizobium sp. CX-Z. Environ. Pollut. 248, 857–864. https://doi.org/10.1016/j.envpol.2019.02.078.

Coplen, T.B., 2011. Guidelines and recommended terms for expression of stable-isotope-ratio and gas-ratio measurement results: guidelines and recommended terms for expressing stable isotope results. Rapid Commun. Mass Spectrom. 25, 2538–2560. https://doi.org/10.1002/rcm.5129.

Czaplicka, M., Barchanska, H., Jaworek, K., Kaczmarczyk, B., 2018. The interaction between atrazine and the mineral horizon of soil: a spectroscopic study. J. Soils Sediments 18, 827–834. https://doi.org/10.1007/s11368-017-1843-9.

De Jonge, L.W., Kjaergaard, C., Moldrup, P., 2004. Colloids and colloid-facilitated transport of contaminants in soils: an introduction. Vadose Zone J. 3, 321–325. https://doi.org/10.2136/vzj2004.0321.

De Souza, A.J., De Araújo Pereira, A.P., Pedrinho, A., Andreote, F.D., Tornisielo, V.L., Tizioto, P.C., Coutinho, L.L., Regitano, J.B., 2022. Land use and roles of soil bacterial community in the dissipation of atrazine. Sci. Total Environ. 827, 154239 https://doi.org/10.1016/j.scitotenv.2022.154239.

De Souza, M.L., Sadowsky, M.J., Wackett, L.P., 1996. Atrazine chlorohydrolase from Pseudomonas sp. strain ADP: gene sequence, enzyme purification, and protein characterization. J. Bacteriol. 178, 4894–4900. https://doi.org/10.1128/jb.178.16.4894-4900.1996.

Devers, M., Azhari, N.E., Kolic, N.-U., Martin-Laurent, F., 2007. Detection and organization of atrazine-degrading genetic potential of seventeen bacterial isolates belonging to divergent taxa indicate a recent common origin of their catabolic functions. FEMS Microbiol. Lett. 273, 78–86. https://doi.org/10.1111/j.1574-6968.2007.00792.x.

Devers, M., Henry, S., Hartmann, A., Martin-Laurent, F., 2005. Horizontal gene transfer of atrazine-degrading genes (atz) fromAgrobacterium tumefaciens St96-4 pADP1:: Tn5 to bacteria of maize-cultivated soil. Pest Manag. Sci. 61, 870–880. https://doi.org/10.1002/ps.1098.

Devers, M., Rouard, N., Martin-Laurent, F., 2008. Fitness drift of an atrazine-degrading population under atrazine selection pressure. Environ. Microbiol. 10, 676–684. https://doi.org/10.1111/j.1462-2920.2007.01490.x.

Devers, M., Soulas, G., Martin-Laurent, F., 2004. Real-time reverse transcription PCR analysis of expression of atrazine catabolism genes in two bacterial strains isolated from soil. J. Microbiol. Methods 56, 3–15. https://doi.org/10.1016/j.mimet.2003.08.015.

Drouin, G., Droz, B., Leresche, F., Payraudeau, S., Masbou, J., Imfeld, G., 2021. Direct and indirect photodegradation of atrazine and S-metolachlor in agriculturally impacted surface water and associated C and N isotope fractionation. Environ. Sci. Process. Impacts. https://doi.org/10.1039/d1em00246e.

Ehrl, B.N., Gharasoo, M., Elsner, M., 2018. Isotope fractionation pinpoints membrane permeability as a barrier to atrazine biodegradation in gram-negative *Polaromonas sp.* nea-C. Environ. Sci. Technol. 52, 4137–4144. https://doi.org/10.1021/acs.est.7b06599.

El-Sebai, T., Lagacherie, B., Cooper, J.F., Soulas, G., Martin-Laurent, F., 2005. Enhanced isoproturon mineralisation in a clay silt loam agricultural soil. Agron. Sustain. Dev. 25, 271–277. https://doi.org/10.1051/agro:2005003.

Elsner, M., Imfeld, G., 2016. Compound-specific isotope analysis (CSIA) of micropollutants in the environment — current developments and future challenges. Curr. Opin. Biotechnol. 41, 60–72. https://doi.org/10.1016/j.copbio.2016.04.014.

Fenner, K., Canonica, S., Wackett, L.P., Elsner, M., 2013. Evaluating pesticide degradation in the environment: blind spots and emerging opportunities. Science 341, 752–758. https://doi.org/10.1126/science.1236281.

Gilevska, T., Wiegert, C., Droz, B., Junginger, T., Prieto-Espinoza, M., Borreca, A., Imfeld, G., 2022. Simple extraction methods for pesticide compound-specific isotope analysis from environmental samples. MethodsX 9, 101880. https://doi.org/10.1016/j.mex.2022.101880.

Hofstetter, T.B., Bakkour, R., Buchner, D., Eisenmann, H., Fischer, A., Gehre, M., Haderlein, S.B., Höhener, P., Hunkeler, D., Imfeld, G., Jochmann, M.A., Kümmel, S., Martin, P.R., Pati, S.G., Schmidt, T.C., Vogt, C., Elsner, M., 2024. Perspectives of compound-specific isotope analysis of organic contaminants for assessing environmental fate and managing chemical pollution. Nat. Water 2, 14–30. https://doi.org/10.1038/s44221-023-00176-4.

Höhener, P., Guers, D., Malleret, L., Boukaroum, O., Martin-Laurent, F., Masbou, J., Payraudeau, S., Imfeld, G., 2022. Multi-elemental compound-specific isotope analysis of pesticides for source identification and monitoring of degradation in soil: a review. Environ. Chem. Lett. 20, 3927–3942. https://doi.org/10.1007/s10311-022-01489-8.

Hussain, S., Devers-Lamrani, M., Spor, A., Rouard, N., Porcherot, M., Beguet, J., Martin-Laurent, F., 2013. Mapping field spatial distribution patterns of isoproturon-mineralizing activity over a three-year winter wheat/rape seed/barley rotation. Chemosphere 90, 2499–2511. https://doi.org/10.1016/j.chemosphere.2012.10.080.

Jablonowski, N.D., Borchard, N., Zajkoska, P., Fernández-Bayo, J.D., Martinazzo, R., Berns, A.E., Burauel, P., 2013. Biochar-mediated [^{14} C]atrazine mineralization in atrazine-adapted soils from Belgium and Brazil. J. Agric. Food Chem. 61, 512–516. https://doi.org/10.1021/jf303957a.

Jablonowski, N.D., Köppchen, S., Hofmann, D., Schäffer, A., Burauel, P., 2009. Persistence of 14C-labeled atrazine and its residues in a field lysimeter soil after 22 years. Environ. Pollut. 157, 2126–2131. https://doi.org/10.1016/j.envpol.2009.02.004.

Jia, W., Shen, D., Yu, K., Zhong, J., Li, Z., Ye, Q., Jiang, J., Wang, W., 2021. Reducing the environmental risk of chlorpyrifos application through appropriate agricultural management: evidence from carbon-14 tracking. J. Agric. Food Chem. 69, 7324–7333. https://doi.org/10.1021/acs.jafc.1c02753.

Kruger, E.L., Somasundaram, L., Coats, J.R., Kanwar, R.S., 1993. Persistence and degradation of [^{14} C]atrazine and [^{14} C]deisopropylatrazine as affected by soil depth and moisture conditions. Environ. Toxicol. Chem. 12, 1959–1967. https://doi.org/10.1002/etc.5620121102.

LeBaron, H.M., McFarland, J.E., Burnside, O.C., 2008. The triazine herbicides: a milestone in the development of weed control technology. In: The Triazine Herbicides. Elsevier, pp. 1–12. https://doi.org/10.1016/B978-044451167-6.50004-0.

Mandelbaum, R.T., Allan, D.L., Wackett, L.P., 1995. Isolation and Characterization of a Pseudomonas sp. That Mineralizes the s-Triazine Herbicide Atrazine. Appl. Environ. Microbiol. 61, 1451–1457. https://doi.org/10.1128/aem.61.4.1451-1457.1995.

Mandelbaum, R.T., Wackett, L.P., Allan, D.L., 1993. Rapid hydrolysis of atrazine to hydroxyatrazine by soil bacteria. Environ. Sci. Technol. 27, 1943–1946. https://doi.org/10.1021/es00046a028.

Mateo-Sagasta, J., Zadeh, S.M., Turral, H., 2017. Water Pollution from Agriculture: A Global Review.

Meyer, A.H., Penning, H., Elsner, M., 2009. C and N Isotope fractionation suggests similar mechanisms of microbial atrazine transformation despite involvement of different enzymes (AtzA and TrzN). Environ. Sci. Technol. 43, 8079–8085. https://doi.org/10.1021/es9013618.

Mudhoo, A., Garg, V.K., 2011. Sorption, transport and transformation of atrazine in soils, minerals and composts: a review. Pedosphere 21, 11–25. https://doi.org/10.1016/S1002-0160(10)60074-4.

Park, J.-H., Feng, Y., Yong Cho, S., Voice, T.C., Boyd, S.A., 2004. Sorbed atrazine shifts into non-desorbable sites of soil organic matter during aging. Water Res. 38, 3881–3892. https://doi.org/10.1016/j.watres.2004.06.026.

Riedo, J., Wettstein, F.E., Rösch, A., Herzog, C., Banerjee, S., Büchi, L., Charles, R., Wächter, D., Martin-Laurent, F., Bucheli, T.D., Walder, F., van der Heijden, M.G.A., 2021. Widespread occurrence of pesticides in organically managed agricultural soils—the ghost of a conventional agricultural past? Environ. Sci. Technol. 55, 2919–2928. https://doi.org/10.1021/acs.est.0c06405.

Rousseaux, S., Hartmann, A., Lagacherie, B., Piutti, S., Andreux, F., Soulas, G., 2003. Inoculation of an atrazine-degrading strain, Chelatobacter heintzii Cit1, in four different soils: effects of different inoculum densities. Chemosphere 51, 569–576. https://doi.org/10.1016/S0045-6535(02)00810-X.

Rousseaux, S., Hartmann, A., Soulas, G., 2001. Isolation and characterisation of new Gram-negative and Gram-positive atrazine degrading bacteria from different French soils. FEMS Microbiol. Ecol. 36, 211–222. https://doi.org/10.1111/j.1574-6941.2001.tb00842.x.

Satsuma, K., 2010. Mineralization of s-triazine herbicides by a newly isolated Nocardioides species strain DN36. Appl. Microbiol. Biotechnol. 86, 1585–1592. https://doi.org/10.1007/s00253-010-2460-3.

Scott, K.M., Lu, X., Cavanaugh, C.M., Liu, J.S., 2004. Optimal methods for estimating kinetic isotope effects from different forms of the Rayleigh distillation equation. Geochim. Cosmochim. Acta 68, 433–442. https://doi.org/10.1016/S0016-7037(03)00459-9.

Shapir, N., Mongodin, E.F., Sadowsky, M.J., Daugherty, S.C., Nelson, K.E., Wackett, L.P., 2007. Evolution of catabolic pathways: genomic insights into microbial *s* -triazine metabolism. J. Bacteriol. 189, 674–682. https://doi.org/10.1128/JB.01257-06.

Singh, S., Kumar, V., Chauhan, A., Datta, S., Wani, A.B., Singh, N., Singh, J., 2018. Toxicity, degradation and analysis of the herbicide atrazine. Environ. Chem. Lett. 16, 211–237. https://doi.org/10.1007/s10311-017-0665-8.

Soulas, G., 1993. Evidence for the existence of different physiological groups in the microbial community responsible for 2,4-d mineralization in soil. Soil Biol. Biochem. 25, 443–449. https://doi.org/10.1016/0038-0717(93)90069-N.

Tappe, W., Groeneweg, J., Jantsch, B., 2002. Diffuse atrazine pollution in German aquifers. Biodegradation 13, 3–10. https://doi.org/10.1023/A:1016325527709.

Torrentó, C., Ponsin, V., Lihl, C., Hofstetter, T.B., Baran, N., Elsner, M., Hunkeler, D., 2021. Triple-element compound-specific stable isotope analysis (3D-CSIA): added value of Cl isotope ratios to assess herbicide degradation. Environ. Sci. Technol. 55, 13891–13901. https://doi.org/10.1021/acs.est.1c03981.

Zwietering, M.H., Jongenburger, I., Rombouts, F.M., Van 'T Riet, K., 1990. Modeling of the bacterial growth curve. Appl. Environ. Microbiol. 56, 1875–1881. https://doi.org/10.1128/aem.56.6.1875-1881.1990.